

SPREAD DOPPLER CLUTTER MITIGATION FOR OTH RADAR BY PHYSICS-ASSISTED ADAPTIVE PROCESSING

Dinesh R, Jeffrey L. Krolik

*Department of Electrical and Computer Engineering,
Duke University, Durham, NC, 27708-0291, USA
dinesh@ee.duke.edu*

As above, jk@ee.duke.edu

ABSTRACT

The detection performance of skywave HF over-the-horizon radars is fundamentally limited by ionospheric motion which causes spreading of surface clutter returns in Doppler space. This paper exploits a model for HF propagation through ionospheric irregularities based on a thin phase screen formulation which is used to derive the Doppler spread and the spatio-temporal dependence in the received field due to ionospheric motion. This paper presents an adaptive space-time processing approach for mitigating the range-coincident main-lobe spread Doppler clutter (SDC). This method exploits the temporal correlation between main-lobe and side-lobe returns of the received field using reference beams for clutter cancellation in directions predicted by the thin-phase screen propagation model. Initial processing on simulated SDC data with injection of a simulated target shows that this approach can provide a target-to-clutter ratio improvement greater than 10 dB.

1. INTRODUCTION

A critical function performed by over-the-horizon radar (OTHR) is to discriminate target returns from those backscattered off the sea by exploiting their different Doppler spectra. Separation of targets depends not only on the velocity of the target but also on the motion of the ionospheric medium. Particularly in equatorial regions, HF propagation through moving ionospheric irregularities occurring after day-night transitions can cause the clutter return to be spread in Doppler space thereby obscuring the presence of targets. Several approaches have been proposed to mitigate different types of spread Doppler clutter (SDC) [3,4,5]. As in [5], our work focuses on reducing “range-coincident” SDC arising from the same range-azimuth resolution cell as the hypothesized target. However, [5] depends on assumptions concerning the spatial correlation of the ionospheric irregularities and the particular orientation of propagation paths relative to the earth’s magnetic field lines. In our model, the ionospheric irregularities are assumed to constitute a random medium moving in the East-West direction with a velocity that can be assumed constant over the coherent integration time (CIT) period of the radar. For a sufficiently thin layer of irregularities, amplitude fluctuations occurring within the layer can be considered negligible, and the ionospheric layer can be replaced by a thin phase screen that imposes only a phase variation and a Doppler on the incident HF wave. In this paper, we first derive the Doppler spread and the field produced on the receiver array by using the phase screen model. We then propose a propagation model and discuss different mechanisms that cause SDC in the received field. Then we derive the received field based on our model and evaluate the spatio-temporal dependence in the received field. Finally, we present a solution to exploit this space-time correlation and to mitigate SDC in the main-lobe of the receiver. In this paper, without loss of generality, we consider the detection of targets that reside in the broad side direction of the receive array and this direction is assumed to be collinear to the main-lobe of the receive beamformer.

2. PHASE SCREEN ANALYSIS

Ionospheric scattering can be reasonably modeled using a thin phase screen if we restrict ourselves to first order scattering in skywave propagation. Thin phase screen modeling, appropriate along raypaths with only moderate ionospheric penetration depths, can be justified for modeling at least some sources of spread Doppler clutter, since attenuation generally increases rapidly along much higher elevation angle rays. The forward problem of calculating the scattered field, on propagation through the phase screen to the receiver array, has usually been solved on the basis of the Huygens-Fresnel approximation [1]. We also have used the same methods, however, we are interested in knowing the space-time statistics of the scattered field rather than deducing statistical properties of the ionospheric irregularities.

If we have a thin phase screen of length L moving with a constant velocity v_s along say x direction in the x - z plane, its transmittance function can be written as sum of several traveling wave exponentials with random amplitudes.

$$P_s(x,t) = \sum_{k_s} \beta(k_s) \exp[jk_s(x - v_s t)] \quad |x| \leq L/2 \quad (1.1)$$

Let the incident field be a plane wave with frequency ω_0 and wave-number k_{ix} along x direction.

$$E_i(x,z,t) = \alpha(k_{ix}) \exp[jk_{ix}x + jk_{iz}z - j\omega_0 t] \quad (1.2)$$

The scattered field at a distance z from the screen can be calculated based on Huygens-Fresnel approximation as

$$E_r(x,z,t) = \frac{1}{j\sqrt{\lambda z}} \int_{-L/2}^{L/2} E_i(\zeta,z,t) P_s(\zeta,t) \exp\left[\frac{j\pi}{\lambda z}(x-\zeta)^2\right] d\zeta \quad (1.3)$$

Carrying out the integration and dropping the factors that depend only on z ,

$$E_r(x,t) = \sum_{k_s} \beta(k_s) \alpha(k_{ix}) \exp[-j(\omega_0 + k_s v_s)t] \exp[j(k_s + k_{ix})x] I_q \quad (1.4)$$

The term I_q represents the Fresnel function resulting from the integration of the quadratic phase functions.

$$I_q(x) = \frac{1}{\sqrt{\lambda z}} \int_{-L/2}^{L/2} \exp\left[\frac{j\pi}{\lambda z} \left(\zeta - x + \frac{\lambda z}{2\pi}(k_{ix} + k_s)\right)^2\right] d\zeta \quad (1.5)$$

Fresnel function I_q limits the spatial frequencies that an array at a distance z can receive from the phase screen. For example, if a 10 km long phase screen is located 1000 km away from the receiver array, the spatial frequencies of the scattered field that reach the array of length 2 km are confined to an angular width of 1.2° . The Fresnel function also imposes a slowly varying amplitude function on the received field, but it can be neglected if we consider only a very narrow beam of field received from the phase screen. The received field at the array can be written as

$$E_r(x,t) = \sum_{k_s} \beta(k_s) \alpha(k_{ix}) \exp[-j(\omega_0 + k_s v_s)t] \exp[j(k_s + k_{ix})x] I_q \quad (1.6)$$

The Doppler frequency $\omega_s = k_s v_s$ associated with the received field is linearly proportional to the scattering spatial frequency k_s of the phase screen. For a receiver array located along a given direction from the phase screen, k_s is dependent on the incident angle (k_{ix}) at the phase screen. Therefore waves incident at different angles on the screen scatter to the receiver with different Dopplers. This mechanism is the principal source of Doppler spread in the clutter return. This is confirmed by the fact that rougher ionosphere causes higher Doppler spread at the receiver.

3. PROPAGATION MODEL FOR OTH RADAR

The radar return at the OTHR receiver contains very strong surface backscatter clutter, accompanied by weak target backscatter and some background atmospheric noise. The surface backscatter, although usually concentrated at zero Doppler frequency, is often modulated by the random time varying nature of the ionosphere, and therefore the ground return is spread in Doppler space. Fig.1 shows the side-view and Fig.2 shows the top-view of the model. In this paper, it is assumed that high elevation ray paths are the ones responsible for Doppler spreading and low elevation angle rays, at more nearly grazing incidence to the ionosphere, are not subject to Doppler spreading. Accordingly, the higher

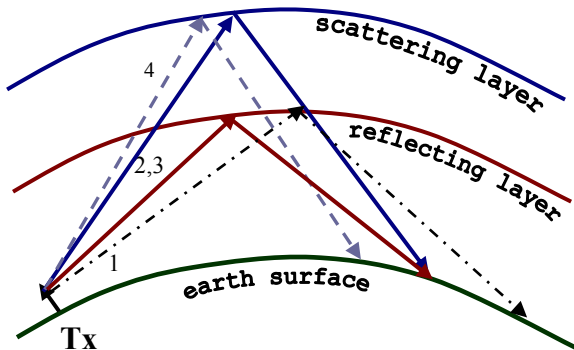


Figure (1): Side-view

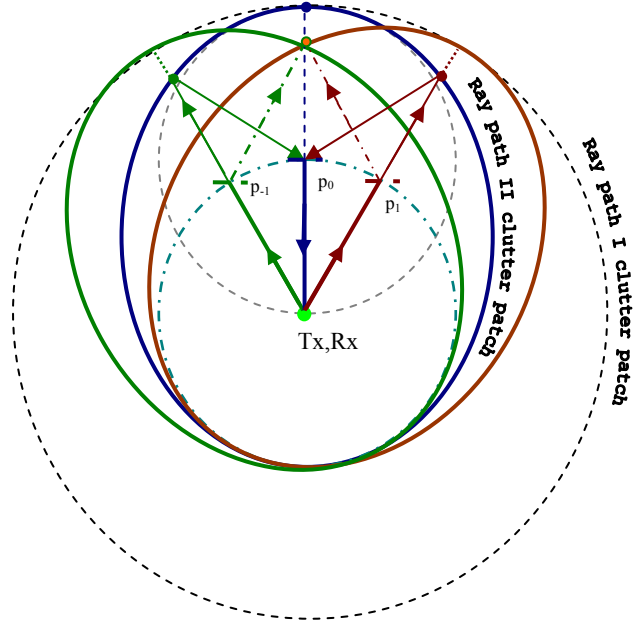


Figure (2): Top-view

elevation angle rays transverse a moving thin phase screen with random irregularities and the low elevation angle rays see essentially a constant (flat) phase screen. Dividing the ionosphere into azimuthal segments, the received field may be computed as the sum of contributions from smaller, finite-length phase screens over a set of azimuthal directions. These phase screens are assumed to be located at a constant slant-range to the radar and are moving East-West with constant speed. The length of the phase screen is chosen to be around 10 km so that the statistical properties of the ionospheric irregularities remain stationary within this length. Even though it is assumed here that the direction of ionospheric motion is parallel to the antenna array axis, the same analysis can be extended for other array orientations too. In the present work, for simplicity, the Transmitter (Tx) and the Receiver (Rx) antenna arrays are assumed to be co-located. Round-trip propagation between Tx and Rx can happen in four different ways considering only the azimuthal directions as shown in Fig.1. The first ray path goes through and comes back via the constant phase screen and is referred to as the direct ray path. The constant phase screen reflects the signal and does not cause any Doppler spread. The second ray path goes through the flat phase screen like the first, but comes back through the scattering phase screen and scatters in the return direction. Doppler spread in the received signal is only due to backward or in-bound scattering. The third ray path goes through the scattering phase screen and scatters in the forward direction, but comes back via the flat phase screen. Doppler spread in the received signal is only due to forward or out-bound scattering. The fourth ray goes through and comes back via the high-altitude scattering phase screen and scatters twice. The received signal exhibits twice the Doppler spread compared to that of 2nd and 3rd ray path and is usually weak because of double scattering. As shown, main contribution to SDC comes from the 2nd and 3rd ray paths and hence only those two paths are considered in our model. For a given Time delay or slant range, the locus of the illuminated clutter patch can be shown to be a circle for the ray paths I and IV and an ellipse for the ray paths II and III. Signal coming from ray path II along the red line (shown in Fig.2) comes from clutter patches on the red ellipse. Tx side-lobe fields that follow ray path II and scatter from clutter patch along the blue ellipse shown in Fig.2, come back in the main-lobe with different Dopplers. Similarly, the Tx main-lobe field that follows ray path III, scatters in the forward direction, illuminates ground along the same blue ellipse and comes back at different side-lobe angles with the associated Dopplers. Thereby, a space-time correlation is introduced in the received field. The relationship between Doppler and side-lobe azimuth can be derived based on the model geometry and phase screen results (1.6). If θ_r is the angle of the received beam (side lobe angle) and θ_s is the scattering angle at the ionospheric phase screen, the equation relating them is

$$\exp(j\theta_r) = \frac{1 + c_z \exp(j\theta_s)}{c_z + \exp(j\theta_s)} \quad (1.7)$$

where z_0 is the slant-distance between Tx and the phase screen, T_p is the total round trip delay of the received signal and $c_z = cT_p / z$, c is the speed of light. Doppler introduced by the scattering is given by $\omega_s = 2\pi v_s \sin(\theta_s) / \lambda$. The Tx side-lobe field traveling along θ_r could also follow ray path III, scatter in the forward direction and come back in the main lobe with a negative Doppler $-\omega_s$ as indicated by dotted red line in Fig. 2. Each Doppler component (ω_s) in the main-lobe field is thus correlated with two side-lobe fields (θ_r and $-\theta_r$) indicated by solid red line and dotted green line in Fig. 2. The main-lobe field can be written as the sum of contributions from these two paths. The received field at the array is then given by

$$E_r(x, t) = \sum_{k_x} \exp(jk_x x) \sum_{k_s} \exp(jk_s v_s t) [\alpha(k_x, k_s) p(k_x, k_s) + \beta(k_x, k_s) q(k_x, k_s)] \quad (1.8)$$

where α and β correspond to scattering coefficients of the clutter and p and q correspond to scattering coefficients of the phase screen. These coefficients are related by (1.7) and (1.6).

4. ADAPTIVE SPACE-TIME PROCESSING

Our objective is to detect moving targets in the main-lobe direction of the receive beampattern. It has been argued in section 3, that the main-lobe clutter is correlated with the side-lobe clutter. The main-lobe SDC is suppressed by exploiting this correlation. For a given side-lobe angle θ_r , Doppler component in the side-lobe field that is correlated with the main-lobe field is computed using (1.7) as $\omega_i = 2\pi v_s \sin(\theta_s) / \lambda$. A Wiener filter is set up to estimate and cancel the main-lobe component that is correlated with the side-lobe field. Let $E_{mb}(t)$ be the temporal response of the received field after beamforming in the main-lobe direction and $E_{s1}(t)$ be the temporal response of the side-lobe field. The side-lobe signal $E_{s1}(t)$ is passed through a narrow band pass filter with center frequency ω_i . The bandwidth of the filter is chosen such that it corresponds to the Doppler spread caused by the finite beam-width of the side-lobe beam.

The Wiener filter is designed with main-lobe signal $E_{mb}(t)$ as the reference and narrowband filtered $E_{s1}(t)$ as the input signal. Output estimate given by Wiener filter of tap length N is

$$\hat{E}_{mb}(t) = \sum_{k=0}^{k=N-1} E_{s1}(t-k) W_0(k) \quad (1.9)$$

By subtracting the Wiener filter estimate from the main-lobe field, clutter in the main-lobe field is reduced. By making use of all the available side-lobe fields, the main-lobe Doppler spread is mitigated.

5. SIMULATION RESULTS

The field at the Rx array is simulated based on the model (1.8). A waveform with approximately 20 Hz repetition frequency and 6 second CIT is used. The simulated target has power 30 dB above the estimated atmospheric noise level and 25 dB less than the clutter peak in the received field. Figure (3) shows the Doppler spectrum of both the received field and the output of the Wiener filter. The injected target cannot be seen in the received field since the clutter return is spread in Doppler. But SDC is suppressed very well in the Wiener filter output and the target peak emerges clearly as the highest value. Our processing yields an average of 10 dB improvement in the target-to-clutter ratio compared to conventional Doppler processing. Our method requires the estimation of approximate slant-height and the relative velocity of ionospheric irregularities which can be done by maximizing the post-processed sub clutter visibility of the data.

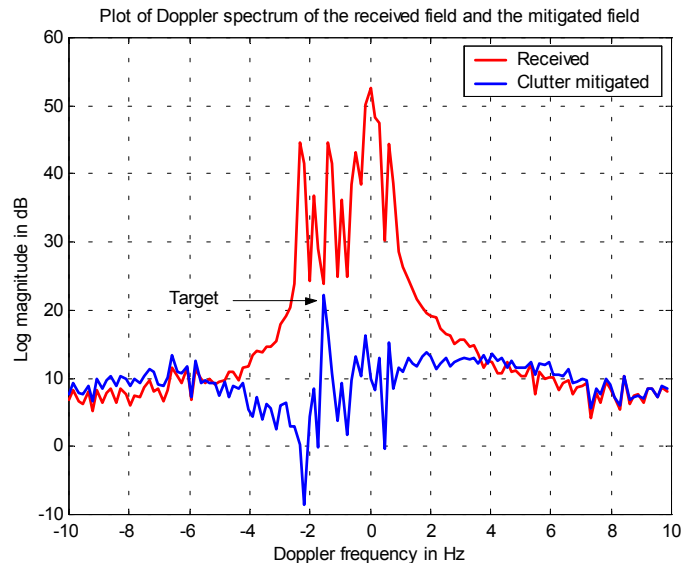


Figure (3): Doppler spectrum

6. CONCLUSIONS

A propagation model for explaining different mechanisms that cause spread Doppler clutter in OTH radar has been proposed. An adaptive space-time processing method aimed at reducing spread Doppler clutter for improved target detection has also been presented. This method uses Wiener filtering to mitigate SDC in the main-lobe of the receive array by exploiting the space-time correlation in the received field caused due to ionospheric motion. Initial processing on simulated spread Doppler clutter data with injection of a simulated target shows that this approach can provide a target-to-clutter ratio improvement greater than 10 dB.

REFERENCES:

- [1] H.G. Booker, J.A. Ratcliffe and D.H. Shinn, "Diffraction from an irregular screen with applications to ionospheric problems," *Philos. Trans. R. Soc. London, Ser. A*, 242, 579-607, 1950.
- [2] C.J. Coleman, "A model of HF sky wave radar clutter," *Radio Science*, vol 31, no. 4, pp. 869-875, July-Aug 1996
- [3] S.J. Anderson and Y.I. Abramovich, "A unified approach to detection, classification and correction of ionospheric distortion in HF sky wave radar systems," *Radio Science*, vol.33, pp. 1055-1067, July-Aug 1998.
- [4] J. Parent and A. Bourdillon, "A method to correct HF sky wave backscattered signals for ionospheric frequency modulation," *IEEE Transaction on Antennas and Propagation*, vol. AP-36, pp. 127-135, 1988.
- [5] Kerem Harmanci and Jeffrey Krolik, "Matched window processing for mitigating over the horizon radar spread Doppler clutter," *Proceedings of the ICAASSP 99 conference*, vol. 5. pp. 2789-2792.